Global Biogeochemical Cycles

RESEARCH ARTICLE
10.1029/2023GB007833

A Spatial Assessment of Current and Future Foliar Hg Uptake Fluxes Across European Forests

Lena Wohlgemuth[1,2], **Aryeh Feinberg**[3], **Allan Buras**[4], **and Martin Jiskra**[1]

[1]Department of Environmental Sciences, University of Basel, Basel, Switzerland, [2]Thünen Institute of Forest Ecosystems, Eberswalde, Germany, [3]Institute for Data, Systems, and Society, MIT, Cambridge, MA, USA, [4]TUM School of Life Sciences, Technical University of Munich, Munich, Germany

Abstract Atmospheric mercury (Hg) is deposited to land surfaces mainly through vegetation uptake. Foliage stomatal gas exchange plays an important role for net vegetation Hg uptake, because foliage assimilates Hg via the stomata. Here, we use empirical relationships of foliar Hg uptake by forest tree species to produce a spatially highly resolved (1 km^2) map of foliar Hg fluxes to European forests over one growing season. The modeled forest foliar Hg uptake flux is 23 ± 12 Mg Hg season^{-1}, which agrees with previous estimates from literature. We spatially compared forest Hg fluxes with modeled fluxes of the chemical transport model GEOS-Chem and find a good overall agreement. For European pine forests, stomatal Hg uptake was shown to be sensitive to prevailing conditions of relatively high ambient water vapor pressure deficit (VPD). We tested a stomatal uptake model for the total pine needle Hg uptake flux during four previous growing seasons (1994, 2003, 2015/2017, 2018) and two climate change scenarios (RCP 4.5 and RCP 8.5). The resulting modeled total European pine needle Hg uptake fluxes are in a range of 8.0–9.3 Mg Hg season^{-1} (min–max). The lowest pine forest needle Hg uptake flux to Europe (8 Mg Hg season^{-1}) among all investigated growing seasons was associated with unusually hot and dry ambient conditions in the European summer 2018, highlighting the sensitivity of the investigated flux to prolonged high VPD. We conclude, that stomatal modeling is particularly useful to investigate changes in Hg deposition in the context of extreme climate events.

Key Points:

- Extreme hot and dry atmospheric conditions have the potential to reduce stomatal uptake of ambient mercury by pine trees in Europe
- Atmospheric drought controls on stomatal mercury uptake should be accounted for in mercury transport models like GEOS-Chem
- Forest foliar mercury uptake fluxes to Europe from a bottom-up model generally agree well with results derived from literature and GEOS-Chem

Supporting Information:

Supporting Information may be found in the online version of this article.

Correspondence to:

L. Wohlgemuth,
lena.wohlgemuth@thuenen.de

Citation:

Wohlgemuth, L., Feinberg, A., Buras, A., & Jiskra, M. (2023). A spatial assessment of current and future foliar Hg uptake fluxes across European forests. *Global Biogeochemical Cycles*, *37*, e2023GB007833. https://doi.org/10.1029/2023GB007833

Received 7 MAY 2023
Accepted 25 SEP 2023

1. Introduction

Mercury (Hg) is a toxic pollutant that is transported globally through the atmosphere and deposited from air to land surfaces mainly through vegetation uptake of ambient gaseous elemental Hg(0) (Demers et al., 2013; Enrico et al., 2016; Feinberg et al., 2022; Jiskra et al., 2015; Obrist et al., 2017). Consequently, vegetation uptake has the potential to lower atmospheric Hg(0) transport and Hg deposition to oceans, where Hg can be methylated and bioaccumulated in marine seafood for human consumption (Zhou et al., 2021). In order to assess and improve the effectiveness of mitigation policies for human exposure, it is thus necessary to advance our understanding of environmental drivers of vegetation Hg(0) uptake, particularly in the context of global change (Sonke et al., 2023).

Global vegetation and soil Hg(0) uptake is estimated at 2,850 ± 500 Mg year^{-1} and primarily driven by forests (Feinberg et al., 2022; Obrist et al., 2021; Zhou et al., 2021). The amount of forest Hg(0) deposition exceeds approximate direct anthropogenic emissions to the air of 2,200 Mg Hg year^{-1} (Sonke et al., 2023). In forests, half of the total Hg(0) net deposition is estimated to be stored in tree foliage, while the other half is estimated to be transferred to vascular tissues (e.g., stem, branches, roots), taken up by understory vegetation (e.g., shrubs, grasses) and nonvascular plants (lichen and mosses) or Hg is directly transferred to the forest floor (Obrist et al., 2021; Zhou & Obrist, 2021; Zhou et al., 2021, 2023). In tree foliage, Hg concentrations increase linearly between foliage emergence and senescence (Blackwell et al., 2014; Laacouri et al., 2013; Pleijel et al., 2021; Rea et al., 2002; Wohlgemuth et al., 2020) implying a net foliar Hg deposition flux, albeit Hg re-emission from foliar surfaces of up to 30% of gross foliage Hg(0) deposition had been observed in a subtropical forest in China (W. Yuan et al., 2019a). The bulk (90%–96%) of Hg is stored in foliage tissues as opposed to leaf surfaces and correlates with leaf stomatal density (Laacouri et al., 2013). Studies on Hg stable isotopes in foliage (Demers et al., 2013; Zhou et al., 2021), enriched isotope tracer experiments (Rutter et al., 2011), the vertical variation of net foliar Hg uptake in forest canopies (Wohlgemuth et al., 2020), and canopy Hg(0) fluxes, that correlate with CO_2 fluxes (Zhou et al., 2023) strongly suggest a diffusive uptake pathway of atmospheric Hg(0) to foliage interiors via the stomata (Liu et al., 2021). In this way, foliar Hg(0) uptake is linked to foliage stomatal aperture for atmospheric gas exchange (Wohlgemuth et al., 2022).

Trees regulate foliage stomatal aperture to balance the inward diffusion of CO_2 for photosynthesis with the risk of desiccation caused by excessive outward diffusion of water vapor (Körner, 2013). The degree of stomatal aperture depends on atmospheric CO_2 levels and hydrological conditions (soil water availability and atmospheric evaporative demand) and varies among foliage-specific traits (age, tree species-specific evolutionary metabolic strategy and water use efficiency) (Körner, 2013). Pine, for instance, is an isohydric tree species capable of closing foliage stomata under warm and dry atmospheric conditions relatively early compared to tree species like oak and spruce (Lagergren & Lindroth, 2002; Zweifel et al., 2007, 2009), resulting in a reduced stomatal conductance for pine needle diffusive gas exchange (Panek & Goldstein, 2001). Consistently, Hg(0) uptake rates by pine needles in Europe were found to be lower at forest sites across Europe, where prolonged warm and dry atmospheric conditions prevailed over a given growing season during daytime (Wohlgemuth et al., 2022).

Species-specific stomatal response strategies to meteorological conditions are particularly relevant for projections of future foliar Hg uptake under climate change. Increasing global atmospheric temperatures driven by rising levels of greenhouse gases will result in an increased frequency of droughts (Grossiord et al., 2020) and higher soil moisture deficits (Berg & Sheffield, 2018; Stocker et al., 2019) in various regions of the world. These climatic conditions may decrease foliar Hg(0) uptake fluxes due to lower stomatal conductance (Wohlgemuth et al., 2022). A reduced plant Hg sink could further be amplified by deforestation and forest diebacks, particularly in the tropics (Allen et al., 2015; Brando et al., 2019; Feinberg et al., 2023). Other regions of the world are projected to become wetter through an increase in precipitation rates under climate change (IPCC, 2021a), which might lead to higher foliage stomatal conductance relative to the present and thus higher foliar Hg uptake. With continuing anthropogenic carbon emissions, an elevated atmospheric CO_2 level might have an antagonizing effect on the foliar stomatal Hg(0) uptake flux: foliar Hg(0) uptake could decline with decreasing stomatal conductance under CO_2 fertilization (Norby & Zak, 2011), or, the opposite, the vegetation sink for Hg(0) could increase with intensified biomass growth and higher soil C contents (Hararuk et al., 2013; Jiskra et al., 2018; H. Zhang et al., 2016). In order to make projections of the foliar Hg uptake flux in the next decades, these climate change impacts need to be further investigated and potentially implemented into global and regional Hg cycle models.

Current and future Hg fluxes are modeled in global chemical transport models (CTMs). CTMs like GEOS-Chem (Selin et al., 2008) apply resistance-based algorithms (Wesely, 2007) for modeling Hg(0) deposition fluxes from the atmosphere to vegetated ecosystems and are often based on parameters like leaf area indices (LAIs), temperature and wind speed. The resistance components for leaf stomata within CTMs commonly represent consensus values optimized to fit observations of Hg deposition velocities over vegetated surfaces (Selin et al., 2008; Smith-Downey et al., 2010; L. Zhang et al., 2009; H. Zhang et al., 2016), without taking stomatal feedback to environmental conditions into account (Khan et al., 2019; Wu et al., 2011). Consequently, forest tree species-specific stomatal responses to climate change at foliage level are not parameterized in CTMs. An additional problem related to CTMs is the uncertainty of modeled Hg(0) deposition fluxes due to insufficient model evaluation against dry deposition measurements (Feinberg et al., 2022). This issue of model validation was highlighted in a recent revision of GEOS-Chem parameterization after matching the GEOS-Chem model design to various experimental Hg(0) deposition measurements, which resulted in a doubling of the modeled global flux of Hg(0) dry deposition to land compared to previous model outcomes (Feinberg et al., 2022).

The goal of this study is twofold. For one, we present a spatially highly resolved map of foliar Hg uptake fluxes to European forests using a bottom-up model, which we compare to mapped forest dry deposition fluxes modeled in the CTM GEOS-Chem. Second, we focus our analysis on foliar Hg uptake fluxes to pine in order to investigate the sensitivity of an empirical stomatal response model to different climatic conditions during past growing seasons and for two climate change projections of the years 2068–2082, in order to outline the potential of incorporating a stomatal response function into CTMs.

2. Materials and Methods

2.1. Description of Data Sets

For creating maps of foliar and pine needle Hg uptake fluxes in Europe applying a bottom-up model (Sections 2.2 and 2.3), we drew on multiple data sources:

- *Foliar Hg data*. A data set of foliar Hg uptake rates was derived from Hg measurements in foliage of tree canopies at 272 forest sites of the UNECE International Co-operative Programme on Assessment and Monitoring

of Air Pollution Effects on Forests (ICP Forests). Forest sites are mostly located in Central and Northern Europe (+737 sites in Austria from the Austrian Bio-Indicator Grid) and harmonized foliage sampling methods were employed. All foliage samples within this data set were harvested at the end of the growing seasons 2015 or 2017. Therefore, average foliage values of 2015/2017 constitute reference values of forest foliar Hg uptake fluxes relative to respective fluxes during investigated years of this study. The data set is publicly available and contains 3,569 foliar Hg concentrations of 23 tree species and is described in detail in Wohlgemuth et al. (2022).

- *Meteorological data*. Values on ambient temperature and relative humidity at surface air pressure (1,000 hPa) in Europe (spatial resolution: 0.25° × 0.25°) originate from ERA5 hourly reanalysis data and were downloaded from the Copernicus Climate Data Store (Hersbach et al., 2018). The applied time frame includes hourly daytime (07:00–18:00 LT) values during the respective growing seasons (April–October) of 1994, 2003, 2015, 2017, and 2018.
- *Climate change data*. Regional climate simulation data of air temperature and relative humidity at 2 m above surface level for the years 2068–2082 and two different climate change scenarios (Representative Concentration Pathway (RCP) 4.5 and RCP 8.5 (IPCC, 2021b)) were obtained from the Coordinated Regional Climate Downscaling Experiment (CORDEX) (Jacob et al., 2020) framework for the European domain with a spatial resolution of 0.11° × 0.11° and a temporal resolution of 3hourly daytime (09:00–18:00 LT) values. For representing a range of different climate model outputs, we calculated average values from multiple regional climate models (RCMs) downscaled from global climate models (GCMs) depending on availability for download from the Copernicus Climate Data Store (C3S, 2022). In total, we incorporated data of 15 combinations of 4 RCMs and 6 GCMs for RCP 4.5 and of 13 combinations of 6 RCMs and 8 GCMs for RCP 8.5 (see Table S3 in Supporting Information S1) for an overview of models and ensemble members.
- *European tree species distribution*. We used a map of spatial proportions of tree species groups per km^2 land area from Brus et al. (2012). For use in calculating pine foliar Hg uptake fluxes (see Section 2.3), we summed up spatial relative abundance values of *Pinus sylvestris*, *Pinus pinaster*, *Pinus nigra*, and *Pinus halepensis* from European forest inventories (Buras & Menzel, 2019; Mauri et al., 2017) and multiplied these pine relative abundances with the respective total forest area per km^2 derived from Brus et al. (2012) to obtain pine areal proportions (i.e., proportion of the surface area of a spatial tile, i.e., covered by pine forest). We performed the same calculation (sum of values of *P. sylvestris*, *P. pinaster*, *P. nigra*, and *P. halepensis* and subsequent multiplication with respective total forest area) to estimate the distribution of pine in Europe under climate change using relative abundance probabilities projected from climate analogs for the time period 2061–2090 and RCP 4.5 and RCP 8.5 by Buras and Menzel (2019).
- *Leaf Area Indices (LAIs) and Leaf Mass per Area (LMA) values*. We used the LAI satellite product (spatial resolution: 330 m) of PROBA-V (Dierckx et al., 2014; Fuster et al., 2020) to upscale foliar Hg uptake rates at each ICP Forests site to foliar Hg uptake fluxes (see Section 2.2), along with average LMA values per tree species from Forrester et al. (2017).

2.2. Calculation of Forest Foliage Hg Uptake Fluxes

We determined forest foliar Hg uptake fluxes to European forests on a 1 km^2 spatial resolution applying three basic computational steps: (a) calculation of tree species-specific daily Hg uptake fluxes per m^2 ground area using a bottom-up model; (b) upscaling of respective foliar Hg fluxes per tree species to the European forested area using the areal distribution of corresponding tree species; (c) multiplication of daily forest foliar Hg uptake fluxes per latitude with latitude-dependent growing season length in order to obtain the forest foliar Hg uptake fluxes over one growing season.

Computational step (1) is based on the premise, that foliar Hg uptake rates are tree species-specific (Laacouri et al., 2013; Pleijel et al., 2021; Wohlgemuth et al., 2022). For this reason, we calculated median daily foliar Hg uptake fluxes per tree species group (see Table S2 in Supporting Information S1 for details on tree species groups) of all forest sites from the foliar Hg data set (Section 2.1). The bottom-up modeling approach for calculating daily foliar Hg uptake fluxes from daily foliar Hg uptake rates is described in detail in Wohlgemuth et al. (2020). Briefly, daily foliar Hg uptake rates per gram foliage dry weight (units of ng Hg $g_{d.w.}^{-1}$ d^{-1}) were multiplied with tree species-specific LMA values (Section 2.1) to obtain daily foliar Hg uptake rates per foliage surface area (ng Hg m_{leaf}^{-2} d^{-1}). Subsequently, values of daily foliar Hg uptake rates per foliage surface area are multiplied with values of LAI (m_{leaf}^{2} m_{ground}^{-2}; Section 2.1), resulting in daily foliar Hg fluxes per unit ground area

(ng Hg m^{-2}_{ground} d^{-1}). LAI values of coniferous forests are relatively constant during the active growing season after the initial growth phase of current-season needles (R. Wang et al., 2017), while LAI values of temperate deciduous forests increase rapidly at the beginning of the growing season (leaf flushing) and climax at peak season (June–August, northern hemisphere) (Q. Wang et al., 2005). For coniferous tree species, we used the maximum LAI value during the constant period at each forest site of the ICP Forests data set to calculate needle foliar Hg uptake fluxes. For deciduous tree species, we calculated foliar Hg uptake fluxes as a temporal sequence at every LAI value available over the growing season and subsequently used median foliar Hg uptake flux values of the growing season. For LAI values larger than 3, we applied a species-specific tree height correction factor, to account for lower foliar Hg uptake fluxes of shaded leaves in the lower canopy (Wohlgemuth et al., 2020) (refer to Table S1 in Supporting Information S1 for utilized tree height correction factors). For coniferous species, we multiplied Hg uptake fluxes of current-season needles with a species-specific needle age correction factor to account for lower Hg uptake rates of older needle age classes (Wohlgemuth et al., 2020) (refer to Table S1 in Supporting Information S1 for utilized needle age correction factors).

Computational step (2) involves the multiplication of the proportion of each tree species per km^2 land area with the respective species-specific median daily foliar Hg uptake fluxes. We matched tree species-specific Hg data with the areal forest distribution of the respective tree species (Brus et al., 2012). In the few cases of rare European tree species, where specific Hg data was lacking, we pooled Hg or forest distribution data by tree species group (see Table S2 in Supporting Information S1 for an overview of matched tree species groups between the two data sets). Subsequently, we added up all tree species-specific daily foliar Hg uptake fluxes within each km^2 and obtained one forest foliar daily Hg uptake flux per km^2.

In computational step (3) we calculated forest foliar Hg uptake fluxes per km^2 and one growing season by multiplying each daily foliar Hg uptake flux per km^2 with the growing season length in days following a simple latitudinal model (CLRTAP, 2017). The latitudinal model of growing season determines a growing season length of 192 days at latitude 50° and decreases by 3.5 days per 1° of latitude moving north and increases by 3.5 days per 1° of latitude moving south. We did not normalize forest foliar Hg uptake fluxes by different atmospheric Hg(0) levels, because ambient Hg(0) measured within the European monitoring programme EMEP (Tørseth et al., 2012) was evaluated to be relatively homogeneous in space in Europe and the growing seasons 2015 and 2017 (Wohlgemuth et al., 2022).

2.3. Calculation of Pine Foliar Hg Uptake Fluxes

In previous research, the impact of relatively high atmospheric water VPD on foliar Hg uptake was assessed for pine, spruce, beech, and oak (Wohlgemuth et al., 2022). For pine, a significant empirical relation of pine needle Hg uptake fluxes with VPD was found: pine needle daily Hg uptake rates (upR_{pine}; ng Hg $g^{-1}_{d.w.}$ d^{-1}) were lower at forest sites, where pine trees experienced high hourly daytime VPD values >1.2 kPa over a relatively long time period during the growing season ($proportion_{dayVPD}$ >1.2 kPa) (Wohlgemuth et al., 2022). The negative correlation of pine needle stomatal Hg uptake with timespan of elevated atmospheric VPD is explained by the hydraulic safety strategy of the isohydric tree species pine, which closes stomata relatively early in response to rising VPD (Section 1). We thus calculated daily foliar Hg uptake rates as a function of VPD exclusively for pine, which accounts for 36% of European forested area of our studied spatial domain. The linear regression of daily foliar Hg uptake rates with $proportion_{dayVPD}$ >1.2 kPa is: $upR_{pine} = 0.116–0.13 \times (proportion_{dayVPD}$ >1.2 kPa) (Wohlgemuth et al., 2022). We applied this linear relationship to calculate the pine foliar Hg uptake rates of the forest area of Europe during four different growing seasons in 1994, 2003, an average of 2015 and 2017, 2018, and projected for the time period 2068–2082 under RCP 4.5 and RCP 8.5 (IPCC, 2021b). Using the August-Roche-Magnus formula (W. Yuan et al., 2019b), we calculated ambient water VPD from daytime values of surface temperature and relative humidity, which are available on an hourly resolution from ERA5 (Hersbach et al., 2018) for past growing seasons and on a 3hourly resolution from EURO-CORDEX (Section 2.1) for simulated climate data. Subsequently, we determined the fraction of daytime hours, during which the VPD was above the threshold of 1.2 kPa during the respective latitudinal growing season length. All calculations involving climate data were performed at sciCORE scientific computing center at University of Basel. We defined growing season length per latitude using a latitudinal model ((CLRTAP, 2017), see Section 2.2). For the time period 2068–2082, we assumed the beginning of the growing season to be 3 days earlier and the end of the growing season to be 3 days later to take increases in growing season length under climate change into account (Garonna et al., 2014; Jeong

Table 1
Comparison of the Bottom-Up Model and GEOS-Chem

	Bottom-up model	GEOS-Chem
Model input parameters	Spatial forest distribution (Brus et al., 2012); leaf area indices (LAIs) (Dierckx et al., 2014; Fuster et al., 2020); leaf mass per area (LMA) (Forrester et al., 2017); meteorological parameter: daytime ambient water VPD (Hersbach et al., 2018); foliar Hg uptake rates (Wohlgemuth et al., 2022)	Spatial forest distribution (Gibbs, 2006); leaf area indices (LAIs) (H. Yuan et al., 2011); atmospheric Hg(0) levels (GEOS-Chem v12.8.1 simulation 2015); meteorological parameters: air temperature, pressure, solar radiation, cloud cover, wind speed (GEOS-FP) (Lucchesi, 2018)
Spatial resolution	1 km × 1 km	0.25 × 0.3125°
Basic methodological approach for Hg flux calculation	Spatial upscaling of measured foliar Hg uptake rates (Wohlgemuth et al., 2020)	In-series calculation of Hg dry deposition velocity from parameterized resistance values (Wesely, 2007)
Foliage stomatal Hg uptake flux component	Calculated for pine based on daytime vapor pressure deficit (VPD) values (Section 2.3)	Calculated within the canopy resistance component as a function of land type, leaf area indices (LAIs), and solar radiation
Model output compared in this study	Tree-species specific forest foliar Hg(0) uptake fluxes	Hg(0) dry deposition fluxes to coniferous and deciduous forest land cover

et al., 2011). The underlying areal distribution of pine is based on European forest inventories and projections of pine abundances based on climate analogs under RCP 4.5 and RCP 8.5 by Buras and Menzel (2019) (see Section 2.1).

2.4. GEOS-Chem Forest Deposition Flux Calculation

GEOS-Chem is a global 3-D CTM, which includes a comprehensive Hg cycle (Selin et al., 2008). Table 1 gives an overview of the methodological approach and input parameters for calculating the respective Hg fluxes of GEOS-Chem and the bottom-up model (Section 2.2), which we compared spatially in this study.

We used an offline version of the GEOS-Chem dry deposition code (Feinberg, 2022) to be able to calculate dry deposition velocities at higher resolution and only for certain land use types (i.e., forest areas). The offline dry deposition code computes deposition velocities applying a resistance-based approach (Y. Wang et al., 1998; Wesely, 2007). Input variables (Table 1) are gridded hourly GEOS-FP meteorological data (e.g., air temperature, wind speed, solar radiation, and cloud cover) and weekly LAI values based on MODIS (H. Yuan et al., 2011) for the year 2015. The model calculates the Hg(0) dry deposition velocity based on species-specific parameters including its biological reactivity ($f_0 = 10^{-5}$) and Henry's Law Constant ($H^* = 0.11$ M atm^{-1}). To isolate the uptake of Hg(0) to forests, we calculated the dry deposition velocity only over coniferous and deciduous land cover types from the Olson land map (Gibbs, 2006). The offline calculations output hourly dry deposition velocities over the European domain at 0.25 × 0.3125° resolution. We converted the calculated Hg(0) deposition velocities to fluxes by multiplying with hourly surface Hg(0) concentrations from a GEOS-Chem v12.8.1 simulation for 2015. For this study, we compared the GEOS-Chem Hg(0) dry deposition fluxes to forests with foliar Hg(0) uptake fluxes calculated using the bottom-up model. For both models, Hg fluxes were averaged over the latitude-dependent growing season length in days and cropped to the same spatial extent. As GEOS-Chem and the bottom-up model differ in their geographic resolution (GEOS-Chem: 0.25° × 0.31° ~ 955 km^2 vs. bottom-up: 1 km^2), we downsampled daily forest foliar Hg uptake fluxes from the bottom-up model through bilinear interpolation.

2.5. Uncertainty Analysis of Foliar Hg Uptake Fluxes

The relative uncertainty value per tree species group depended on propagated uncertainties of calculation parameters used to derive the respective foliar Hg uptake flux per tree species group (see Table S4 in Supporting Information S1 for details and values). Subsequently, we calculated one relative uncertainty value per geographic tile of our European flux map (Figure 1) by summarizing the relative uncertainty of each foliar Hg uptake flux per tree species group within each tile according to error propagation principles (Ku, 1966; Papula, 2003). We obtained the relative uncertainty for the total foliar Hg uptake flux to European forests (Figure 1) by propagating all relative uncertainty values per tile. The final relative uncertainty value of total foliar Hg uptake flux to European forests and the reference growing seasons 2015/2017 is 0.52.

3. Results and Discussion

3.1. Spatial Distribution of Forest Foliar Hg Uptake Fluxes Across Europe

Figure 1 visualizes forest foliar Hg uptake fluxes per growing season at a spatial resolution of 1 km^2 (g Hg km^{-2} season^{-1}) in Europe. Forest foliar Hg uptake fluxes generally follow a spatial distribution of European forests, because this map (Figure 1) is based on the proportion of forest tree species per land area (Brus et al., 2012). Consequently, the largest forest foliage Hg uptake fluxes in terms of area are in Fennoscandia (defined here as Norway, Sweden, and Finland) with dense forest land cover of mostly pine and spruce (Brus et al., 2012). Outside of Fennoscandia, forest foliage Hg uptake fluxes fall along large contiguous forested areas, for example,

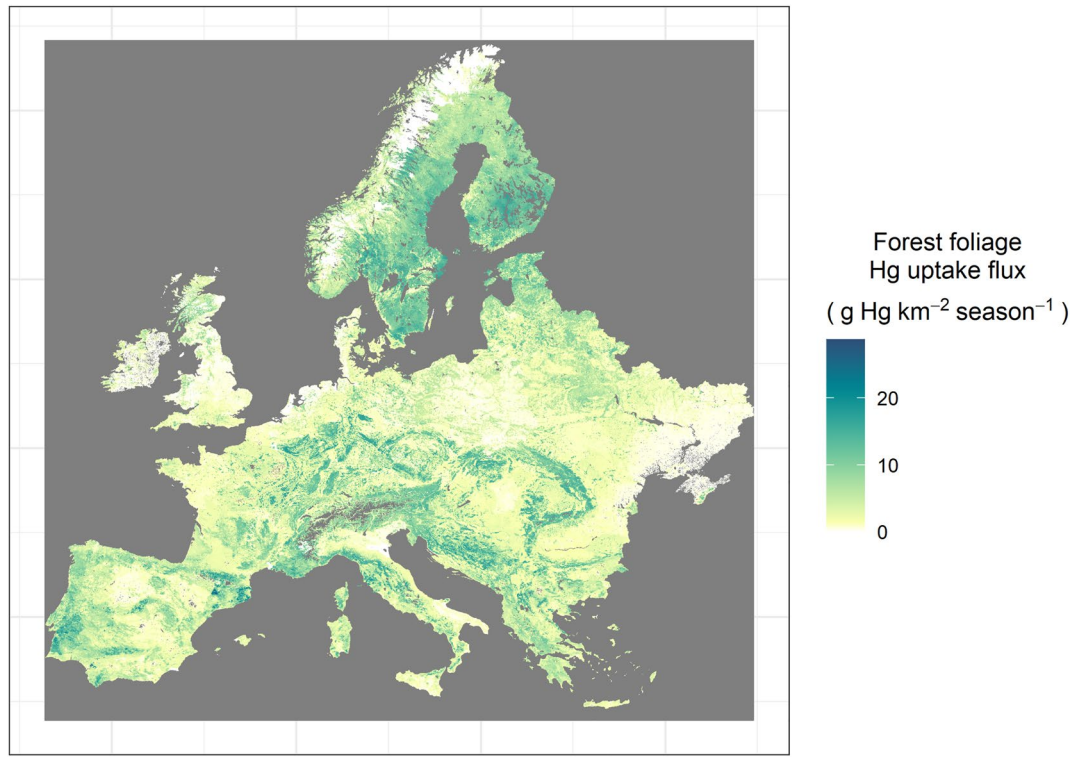

Figure 1. Spatial distribution of forest foliar Hg uptake fluxes (g Hg km^2 growing season^{-1}) to Europe based on a bottom-up extrapolation of foliar Hg concentrations, that were measured and averaged over the 2015 and 2017 growing seasons. Dark gray areas represent excluded non-forested areas (e.g., surface waters or mountain areas).

in the Carpathian Mountains (located in most parts in Romania and Slovakia), the South-Eastern Alps (mostly in Austria, Slovenia, and Italy), the Balkans, or forested low mountain areas like the Black Forest (Germany). By magnitude, forest foliar Hg uptake fluxes (Figure 1) agree well with annual canopy Hg(0) deposition of two temperate forests (14.3 and 15.4 μg m^{-2}) in North America, which were measured by applying a micrometeorological method (Zhou et al., 2023).

The sum of forest foliar Hg uptake fluxes over the land area of Europe (compare Figure 1) equals 23 ± 12 Mg Hg season^{-1}. This total flux is in the same range as a previous estimate of the total foliar Hg uptake flux to Europe (20 ± 3 Mg Hg over the 2018 growing season) based on foliar Hg uptake fluxes at four forested sites (Wohlgemuth et al., 2020). Zhou and Obrist (2021) evaluated a median global foliar Hg assimilation of 28 Mg yr^{-1} for deciduous broadleaf forests and 61 Mg yr^{-1} for evergreen needleleaf forests by combining foliar Hg concentrations with annual net foliar biomass production data of the respective forest types. From these global assimilation estimates by Zhou and Obrist (2021), we calculated a total foliar Hg assimilation of 29 Mg yr^{-1} to the deciduous and coniferous forest land area of Europe (for details see Text S1 in Supporting Information S1), which is slightly higher but still within the uncertainty of the 23 ± 12 Mg Hg season^{-1} from this study. However, foliar Hg uptake fluxes based on net primary foliar biomass production by Zhou and Obrist (2021) does not correct for lower foliar Hg uptake rates by shade leaves and multiyear old needles (see Section 2.2) relative to sun leaves and younger needles (Wohlgemuth et al., 2020), likely resulting in a systematic over-estimation. We assume, that the different time reference (seasonal vs. annual) of the flux from this study (23 ± 12 Mg Hg season^{-1}) and the flux derived from Zhou and Obrist (2021) (29 Mg Hg yr^{-1}) only plays a minor role for explaining the difference between the two fluxes, since we expect a small net foliar biomass production in Europe in winter outside of the growing season. Results from micrometeorological Hg measurements in two temperate forests in North America show, that Hg(0) uptake during the active growing season dominates annual Hg(0) deposition (Zhou et al., 2023). Please note, that from a whole forest ecosystem perspective, fluxes displayed in Figure 1 are exclusively constrained to foliar Hg uptake and do not represent potential Hg fluxes to other ecosystem compartments like forest floor (Zhou et al., 2023).

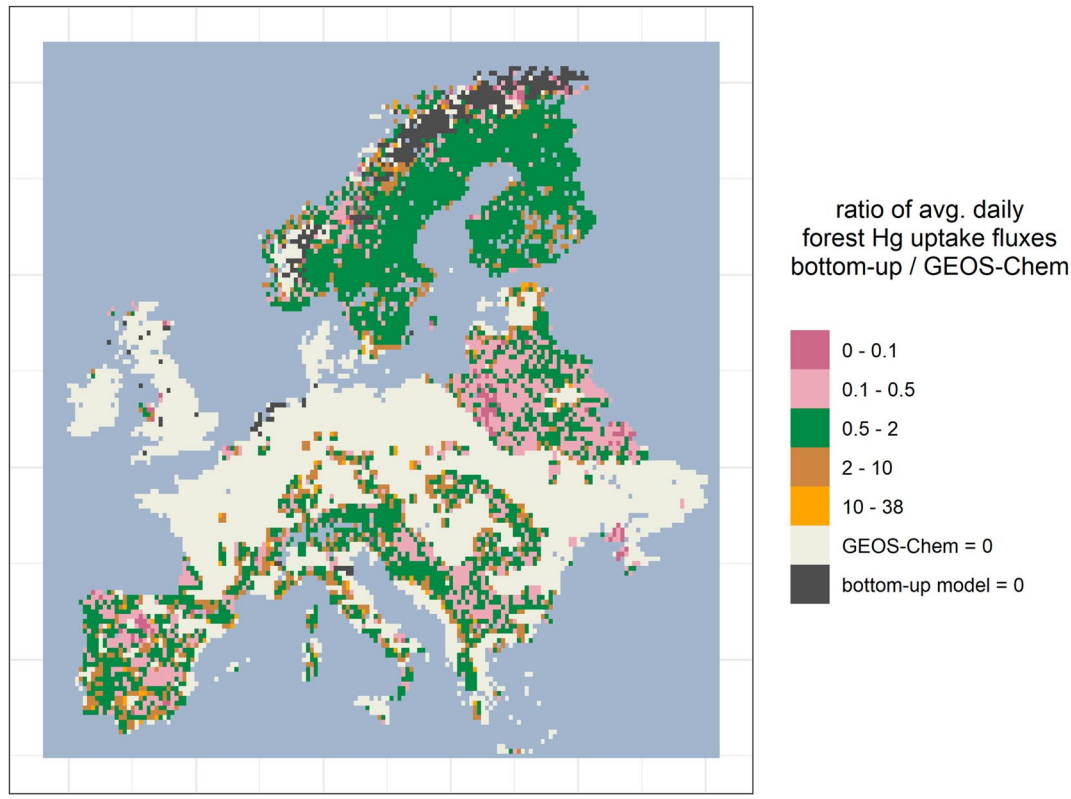

Figure 2. Ratios per spatial unit of daily forest Hg uptake fluxes averaged over the latitude-specific growing season length of the bottom-up model to GEOS-Chem.

3.2. Comparison of Bottom-Up Model With GEOS-Chem

Figure 2 depicts spatial ratios of daily forest Hg uptake fluxes of the bottom-up model to GEOS-Chem. Absolute difference values of the two model outputs are shown in Figure S2 Supporting Information S1.

The overall foliar Hg uptake flux to the total European forested area (Figures 1 and 2) was 22 Mg Hg season^{-1} for GEOS-Chem, which almost equals the total flux of 23 ± 12 Mg Hg season^{-1} for the bottom-up model (Section 3.1). Results of average daily foliar Hg uptake fluxes from GEOS-Chem and the bottom-up model were geographically comparable: In 59% of the spatial domain with values >0, average daily foliar Hg uptake fluxes from the two models differed by factor of 1–2 from each other, in 37% of the domain, model values differed by a factor of 2–10 from each other, and in 4% of the domain respective values differed by a factor of >10 from each other (Figure 2). We examined if differences in modeled average daily foliar Hg uptake fluxes at the same geographic location originate from differences in the underlying forest distribution maps of the two compared models. In 78% of spatial tiles with values >0, the ratio of average daily foliar Hg uptake fluxes of the bottom-up model to GEOS-Chem agreed in range (Figure 2) with the ratio of the forest fraction of the bottom-up model to GEOS-Chem per respective spatial tile. We thus find that the bottom-up model and GEOS-Chem generally produce similar forest Hg flux values per spatial unit given the same forest distribution. This spatial consistency of model outputs is surprising, as the bottom-up model is specific for foliar Hg(0) uptake fluxes based on a wide set of European field data, while GEOS-Chem broadly computes Hg(0) dry deposition fluxes to forests (Table 1). Reasons for minor differences in model outputs are challenging to identify, due to the different approaches, parameters, and underlying maps of the two models (Section 2.4). For future assessment of model accuracy, we therefore suggest to compare model results to actual measurements of the forest foliar Hg uptake flux (Feinberg et al., 2022; Obrist et al., 2021; Zhou et al., 2023).

3.3. Pine Foliar Hg Uptake Fluxes Under Different VPD Scenarios

Figure 3 shows total pine forest foliar Hg uptake fluxes to Europe calculated under different conditions of atmospheric surface-level water VPD during four past growing seasons (1994, 2003, 2015/2017, 2018) and simulated for the years 2068–2082 as an average of multiple climate model outputs (see Section 2.2) under two

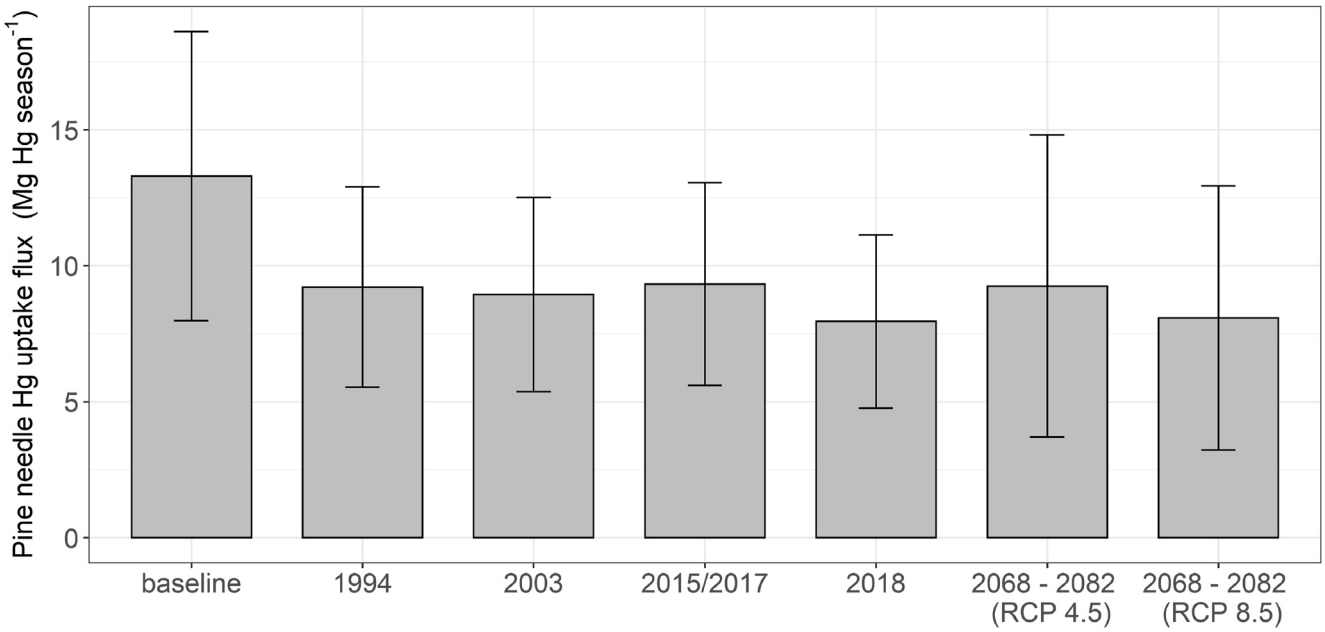

Figure 3. Pine needle Hg uptake flux to European pine forests (Mg Hg season^{-1}) calculated from atmospheric surface water vapor pressure deficit (VPD) conditions during the growing seasons 1994, 2003, 2015/2017, 2018 and projected for the years 2068–2082 under RCP 4.5 and RCP 8.5. Bar on the left represents a baseline pine forest needle Hg uptake flux with no VPD exceedance of 1.2 kPa throughout the growing season.

different climate change scenarios (RCP 4.5 and RCP 8.5). The leftmost bar (Figure 3) represents a theoretical baseline pine needle Hg uptake flux in absence of VPD induced stomatal control (potential maximum transpiration rates) on the pine needle Hg uptake flux. The total pine needle Hg uptake flux to Europe during the reference growing season 2015/2017 (Section 2.2) is 9.3 ± 3.7 Mg Hg representing 70% of the baseline flux of 13.3 ± 5.3 Mg Hg season^{-1}. Thus, based on the pine needle Hg uptake model used in this study (Section 2.3), the VPD effect reduces the total pine needle Hg uptake flux to Europe by approximately 30%.

The relative standard deviation of modeled total pine needle Hg uptake fluxes for the investigated growing seasons (1994, 2003, 2015/2017, 2018, 2068–2082) was 0.07 Mg Hg season^{-1}. Consequently, modeled total European pine needle Hg uptake fluxes hardly differed from each other among growing seasons. The total pine needle Hg uptake flux in Europe depend on VPD conditions in areas where pine forests prevail. Pine forests are primarily located in Northern Europe (Figure S1 in Supporting Information S1). Pine forests located at latitudes >55.3°N account for 21% of the total foliar Hg uptake flux to Europe during the reference growing season (Figure 1). In Northern Europe, hourly ambient VPD was >1.2 kPa during 30% or less of daytime in the growing seasons 1994, 2003, and 2015/2017 due to relatively cool and moist ambient conditions as compared to Central and Southern Europe (see e.g., VPD conditions during reference time period 2015/2017 Figure 4a). In contrast to previous years, the European summer hydrological condition of 2018 has been described as an intense hot drought, during which pronounced stomatal closure of coniferous forests in response to high VPD were recorded in Switzerland (Gharun et al., 2020). In Southern Fennoscandia, conditions of ambient hourly VPD > 1.2 kPa prevailed over exceptionally long time proportions (around 40%) during the summer of 2018 (see Figures 4b and Buras et al., 2020). As a result, the modeled total pine needle Hg uptake flux in Europe in 2015/2017 (9.3 Mg Hg season^{-1}) was by a factor of 1.16 higher than the respective flux in 2018 (8.0 Mg Hg season^{-1}). We conclude, that hot and dry summer conditions (Figure 3) in Fennoscandia crucially impact modeled past total pine needle Hg uptake fluxes in Europe. According to the model results, an average amount of 1.3 Mg Hg was not deposited via pine needle uptake in 2018 compared to 2015/2017, potentially remaining in the atmosphere, where it can be long-range transported to the ocean (Zhou et al., 2021). These 1.3 Mg Hg are more than three times larger than the reported anthropogenic Hg emissions of Sweden in 2021 (Naturvårdsverket, 2023), highlighting the quantitative impact, that hot droughts can have on the pine needle Hg uptake flux.

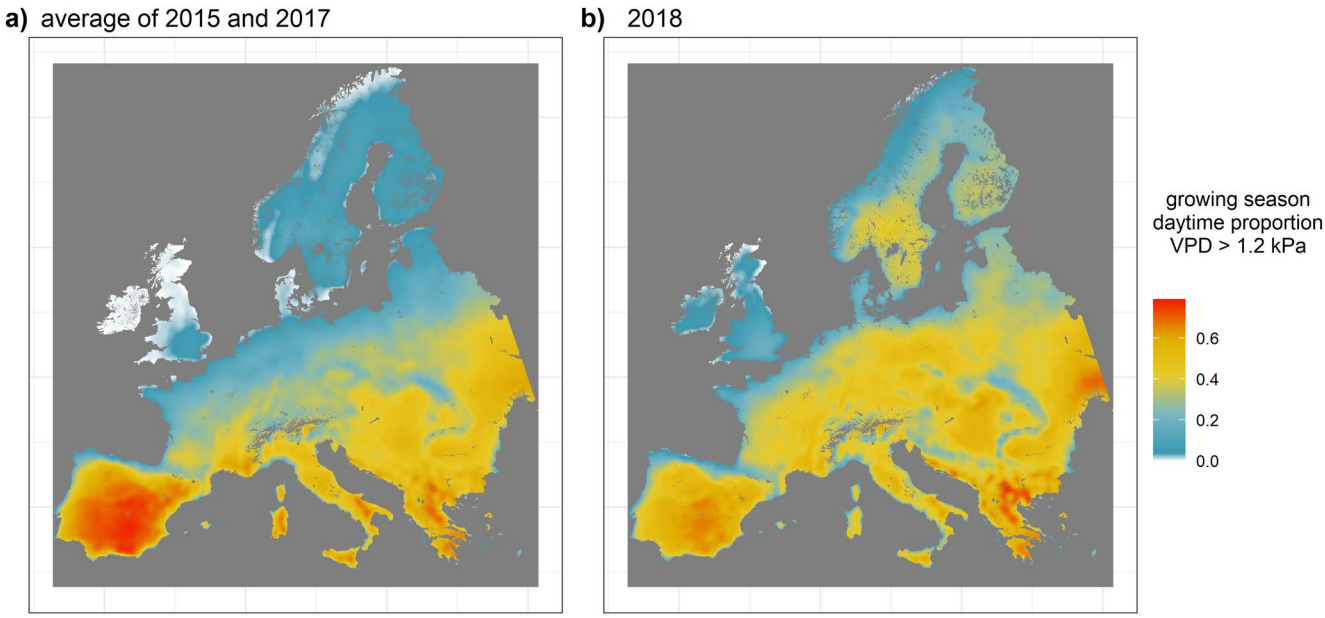

Figure 4. Average daytime proportion of surface level atmospheric water VPD > 1.2 kPa during (a) the reference growing season 2015/2017, and (b) the growing season 2018. All VPD values were calculated from hourly reanalysis data of ERA5 ambient air temperature and relative humidity (Section 2.1).

3.4. Projected Pine Forest Needle Hg Uptake Fluxes Under Climate Change Scenarios

The projected total pine forest needle Hg uptake flux for 2068–2082 (RCP 4.5: 9.3 ± 5.5 Mg Hg season^{-1}; RCP 8.5: 8.1 ± 4.9 Mg Hg season^{-1}) was in the same range as the corresponding average flux for the years 1994, 2003, 2015 and 2017 of 9.1 ± 0.2 Mg Hg season^{-1} (mean ± sd), but slightly higher than the corresponding flux in the year of 2018 (8.0 ± 3.2 Mg Hg season^{-1}), during which Fennoscandia experienced a summer of relatively long hot and dry ambient conditions. Figure 5 maps the absolute deviation of the pine forest needle Hg uptake flux projected for 2068–2082 (simulated future flux) from the corresponding 2018 flux in Europe. Under RCP 4.5, the simulated future flux is higher (blue area in Figure 5a) than the 2018 flux in 65% of total area. Under RCP 8.5,

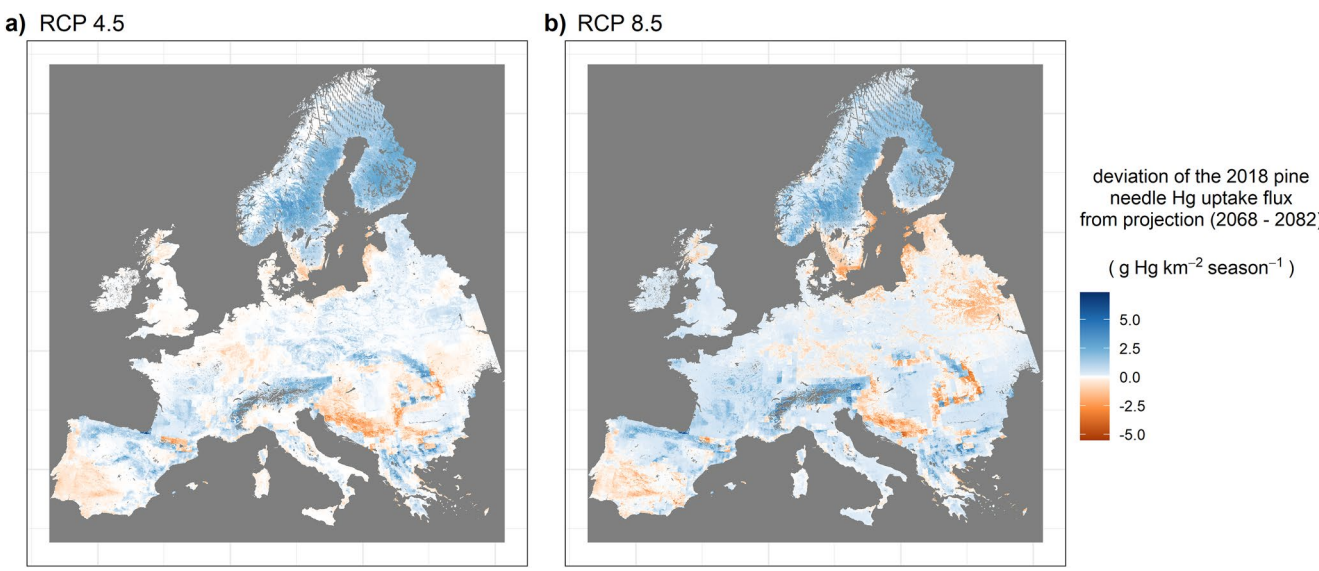

Figure 5. Absolute deviation of projected pine forest foliar Hg uptake fluxes for 2068–2082 (under RCP 4.5 (a) and RCP 8.5 (b)) from the corresponding flux modeled for 2018. In blue areas, the projected future flux under the two climate change scenarios is higher than the respective 2018 flux, in orange areas, this deviation is reversed.

the simulated future flux is higher (blue area in Figure 5b) than the 2018 flux in 43% of total area. In most area of Fennoscandia, where a majority of pine forests in Europe are located (Figure S1 in Supporting Information S1), the future flux is projected to be larger than in 2018. For both climate change scenarios, the projection predicts lower pine needle Hg fluxes to the Balkans and to the Southern Iberian Peninsula than in 2018 (Figure 5).

The pine forest needle Hg uptake flux for 2068–2082 simulated here is a function of both modeled ambient VPD conditions during the growing season and the projected distribution of pine forests in Europe depending on climate analogs (Buras & Menzel, 2019). While the pine forest cover in Southern Sweden is projected to decrease under the climate change scenarios RCP 4.5 and RCP 8.5 from around 50% km^{-2} to around 25% km^{-2}, forest cover in Central and Northern Fennoscandia is projected to be relatively steady for climate analogs of both climate change scenarios (compare Figures S1a–S1c in Supporting Information S1). Average long-term precipitation rates are projected to increase in Scandinavia, along with a decrease of meteorological drought in the coming decades under different climate change scenarios (Forzieri et al., 2014; Kellomäki et al., 2018; Samaniego et al., 2018), which could result in an increase of atmospheric humidity and a decrease of VPD in northern Europe (Oksanen et al., 2019). Under this scenario of wetter forest environments, the Hg sink of Scandinavian pine forest needles would not be significantly diminished. However, drought trends in Fennoscandia are still inconsistent and extreme drought events like in 2018 might occur more frequently under the current rate of climate change (IPCC, 2021a). The summer of 2018 was a record hot drought in Europe (Buras et al., 2020), while climate simulations for 2068–2082 are averaged over multiple climate models (Table S3 in Supporting Information S1), possibly averaging out extreme events. In a scenario, where the maximum proportion of daytime VPD > 1.2 kPA per growing season averaged over 2068–2082 prevails at each spatial unit, the total pine forest needle Hg uptake flux to Europe reduces to 6.9 Mg Hg $season^{-1}$ for RCP 4.5 and 5.0 Mg Hg $season^{-1}$ for RCP 8.5, which corresponds to 74% and 62% of the respective flux derived from an average VPD daytime proportion. We therefore suggest that extreme climate events of extended time periods of ambient daytime VPD > 1.2 kPa like during the growing season 2018 (Figure 4b) could reduce the pine forest needle Hg uptake flux in Fennoscandia in future even compared to average long-term VPD projections (Figure 5).

A source of model uncertainty of the future forest foliar Hg uptake flux under climate change arises from atmospheric Hg(0) concentrations that depend on anthropogenic emissions, re-emissions of mobilized legacy Hg and future global deposition fluxes under climate and land use change (Feinberg et al., 2023; Sonke et al., 2023), which we could not account for in this study. However, our model outputs call attention to the sensitivity of the pine needle Hg uptake flux to extreme hot and dry ambient conditions, which should be accounted for in CTMs under varying atmospheric Hg(0) levels. Going forward, the climate feedback of stomatal Hg(0) drawdown from the atmosphere should likewise be parameterized in CTMs for other tree species but pine. Temperate tree species like oak and beech also react to increasing VPD with stomatal closure (Grossiord et al., 2020; Wohlgemuth et al., 2022), albeit less instantaneously than pine (Cárcer et al., 2018; Martínez-Ferri et al., 2000; Zweifel et al., 2007), which merits further investigation in field and laboratory experiments in the context of foliar Hg uptake and climate change.

The impact of the hot and dry conditions on the pine Hg uptake fluxes might have implications for Hg inputs into aquatic ecosystems. In a recent review on Hg cycling in the context of global change Sonke et al. (2023) highlighted the potential of legacy Hg (i.e., actively cycling Hg that was mobilized in the past) to cause contamination by mobilization of Hg from soils to wetlands and coastal ecosystems via riverine systems. While most soil Hg enters riverine systems by soil erosion from agricultural lands, contaminated sites, and deforested woodland (Panagos et al., 2021; Sonke et al., 2023), a reduced forest foliar Hg uptake and subsequent deposition to forest soils may decrease the amount of runoff Hg from forest soils in the long-term, while long-range Hg transport to the open ocean via the atmosphere might be enhanced (Zhou et al., 2021).

4. Conclusion

We created a highly resolved (1 km^2) map (Figure 1), which visualizes the spatial variation of foliar Hg uptake fluxes to European forests. The highest foliar Hg uptake fluxes are in Fennoscandia, in densely forested areas of Central and Southern Europe, for example, the Carpathian Mountains, the Balkans, or in multiple low mountain areas. We suggest, that this map (Figure 1) can guide decisions on European background Hg monitoring of the terrestrial environment. The total forest foliar Hg uptake flux over the course of one growing season agrees well with Hg flux estimates derived from literature and from the CTM GEOS-Chem for the same land area of Europe

(Figure 2). This precision among modeling results on a European scale using different approaches gives us confidence that the bottom-up model is overall able to represent the seasonal forest foliar Hg uptake flux.

Using an empirical relationship between Hg needle uptake rates of pine trees and VPD threshold exceedance, we found a reduction in modeled pine forest needle Hg uptake flux during the relatively hot and dry growing season in Fennoscandia in 2018 compared to the growing seasons in 1994, 2003, and 2015/2017 (Figure 3). The modeled average amount of Hg, that was not deposited via pine needle uptake in 2018 compared to the reference time period of 2015/2017 exceeded the reported anthropogenic Hg emissions of Sweden in 2021, highlighting the quantitative significance of stomatal Hg uptake. If these hot summer droughts occurred more frequently in Fennoscandia under climate change, the pine forest needle Hg uptake flux would be diminished while these extreme conditions prevail, potentially increasing the Hg burden of the ocean via long-range atmospheric transport. In order to better represent the impact of extreme climate events on the pine forest needle Hg uptake flux, we therefore advise to incorporate a stomatal component of the pine needle Hg uptake flux into CTMs like GEOS-Chem.

Data Availability Statement

Calculated forest foliar Hg uptake fluxes to Europe (Figure 1) and GEOS-Chem simulation data aggregated to seasonal values are publicly available for download from Zenodo at https://zenodo.org/record/7851718#.ZFUeLM5Bw2w and https://zenodo.org/record/7900753#.ZFUgqM5Bw2w respectively. All input data sets to the bottom-up model are described in detail in Section 2.1, along with their respective publications and databases, from which the data sets can be accessed. The offline dry deposition code from GEOS-Chem is accessible for download (Feinberg, 2022). All calculations and visualizations were done in R, Version 4.0.3.

Acknowledgments
L. Wohlgemuth and M. Jiskra acknowledge financial support from the Swiss National Science Foundation (Grant 174101). A. Feinberg acknowledges financial support from the Swiss National Science Foundation (Early Postdoc. Mobility Grant: 195424) and the US National Science Foundation (#1924148). The GEOS-FP data used in this study have been provided by the Global Modeling and Assimilation Office (GMAO) at NASA Goddard Space Flight Center. The evaluation was partly based on data that was collected by partners of the official UNECE ICP Forests Network (http://icp-forests.net/contributors). Part of the ICP Forests data was co-financed by the European Commission. ERA5 and CORDEX data were obtained from the Copernicus Climate Change Service (C3S) Climate Data Store (https://cds.climate.copernicus.eu/cdsapp#!/home). PROBA-V leaf area index values were downloaded from the VITO Product Distribution Portal. Climate calculations under two climate change scenarios (Figures 3 and 4) were performed at sciCORE (http://scicore.unibas.ch/) scientific computing center at University of Basel. Open Access funding enabled and organized by Projekt DEAL.

References

Allen, C. D., Breshears, D. D., & McDowell, N. G. (2015). On underestimation of global vulnerability to tree mortality and forest die-off from hotter drought in the Anthropocene. *Ecosphere*, *6*(8), art129. https://doi.org/10.1890/ES15-00203.1

Berg, A., & Sheffield, J. (2018). Climate change and drought: The soil moisture perspective. *Current Climate Change Reports*, *4*(2), 180–191. https://doi.org/10.1007/s40641-018-0095-0

Blackwell, B., Driscoll, C., Maxwell, J., & Holsen, T. (2014). Changing climate alters inputs and pathways of mercury deposition to forested ecosystems. *Biogeochemistry*, *119*(1–3), 215–228. https://doi.org/10.1007/s10533-014-9961-6

Brando, P. M., Paolucci, L., Ummenhofer, C. C., Ordway, E. M., Hartmann, H., Cattau, M. E., et al. (2019). Droughts, wildfires, and forest carbon cycling: A pantropical synthesis. *Annual Review of Earth and Planetary Sciences*, *47*(1), 555–581. https://doi.org/10.1146/annurev-earth-082517-010235

Brus, D. J., Hengeveld, G. M., Walvoort, D. J. J., Goedhart, P. W., Heidema, A. H., Nabuurs, G. J., & Gunia, K. (2012). Statistical mapping of tree species over Europe. *European Journal of Forest Research*, *131*(1), 145–157. https://doi.org/10.1007/s10342-011-0513-5

Buras, A., & Menzel, A. (2019). Projecting tree species composition changes of European forests for 2061–2090 under RCP 4.5 and RCP 8.5 scenarios. *Frontiers in Plant Science*, *9*(1986). https://doi.org/10.3389/fpls.2018.01986

Buras, A., Rammig, A., & Zang, C. S. (2020). Quantifying impacts of the 2018 drought on European ecosystems in comparison to 2003. *Biogeosciences*, *17*(6), 1655–1672. https://doi.org/10.5194/bg-17-1655-2020

C3S. (2022). Copernicus climate change service (C3S), climate data store (CDS): CORDEX regional climate model data on single levels. Copernicus. https://doi.org/10.24381/cds.bc91edc3

Cárcer, P. S. D., Vitasse, Y., Peñuelas, J., Jassey, V. E. J., Buttler, A., & Signarbieux, C. (2018). Vapor–pressure deficit and extreme climatic variables limit tree growth. *Global Change Biology*, *24*(3), 1108–1122. https://doi.org/10.1111/gcb.13973

CLRTAP. (2017). *Revised chapter 3 of the manual on methodologies and criteria for modelling and mapping critical loads and levels and air pollution effects, risks and trends: Mapping critical levels for vegetation*. Umweltbundesamt. Retrieved from https://www.umweltbundesamt.de/en/manual-for-modelling-mapping-critical-loads-levels

Demers, J. D., Blum, J. D., & Zak, D. R. (2013). Mercury isotopes in a forested ecosystem: Implications for air-surface exchange dynamics and the global mercury cycle. *Global Biogeochemical Cycles*, *27*(1), 222–238. https://doi.org/10.1002/gbc.20021

Dierckx, W., Sterckx, S., Benhadj, I., Livens, S., Duhoux, G., Van Achteren, T., et al. (2014). PROBA-V mission for global vegetation monitoring: Standard products and image quality. *International Journal of Remote Sensing*, *35*(7), 2589–2614. https://doi.org/10.1080/01431161.2014.883097

Enrico, M., Roux, G. L., Marusczak, N., Heimbürger, L.-E., Claustres, A., Fu, X., et al. (2016). Atmospheric mercury transfer to peat bogs dominated by gaseous elemental mercury dry deposition. *Environmental Science & Technology*, *50*(5), 2405–2412. https://doi.org/10.1021/acs.est.5b06058

Feinberg, A. (2022). Code reference: Arifein/offline-drydep: Offline dry deposition model from GEOS-Chem v1.0 (v1.0). *Zenodo*. https://doi.org/10.5281/zenodo.6498126

Feinberg, A., Dlamini, T., Jiskra, M., Shah, V., & Selin, N. E. (2022). Evaluating atmospheric mercury (Hg) uptake by vegetation in a chemistry-transport model. *Environmental Sciences: Processes & Impacts*, *24*(9), 1303–1318. https://doi.org/10.1039/D2EM00032F

Feinberg, A., Jiskra, M., Borrelli, P., Biswakarma, J., & Selin, N. E. (2023). Land use change as an anthropogenic driver of mercury pollution. EarthArXiv preprint. https://doi.org/10.31223/X5TQ03

Forrester, D. I., Tachauer, I. H. H., Annighoefer, P., Barbeito, I., Pretzsch, H., Ruiz-Peinado, R., et al. (2017). Generalized biomass and leaf area allometric equations for European tree species incorporating stand structure, tree age and climate. *Forest Ecology and Management*, *396*, 160–175. https://doi.org/10.1016/j.foreco.2017.04.011

Forzieri, G., Feyen, L., Rojas, R., Flörke, M., Wimmer, F., & Bianchi, A. (2014). Ensemble projections of future streamflow droughts in Europe. *Hydrology and Earth System Sciences*, *18*(1), 85–108. https://doi.org/10.5194/hess-18-85-2014

Fuster, B., Sánchez-Zapero, J., Camacho, F., García-Santos, V., Verger, A., Lacaze, R., et al. (2020). Quality assessment of PROBA-V LAI, fAPAR and fCOVER collection 300 m products of Copernicus global land service. *Remote Sensing*, *12*(6), 1017. https://doi.org/10.3390/rs12061017

Garonna, I., Jong, R. D., Wit, A. J. W. D., Mücher, C. A., Schmid, B., & Schaepman, M. E. (2014). Strong contribution of autumn phenology to changes in satellite-derived growing season length estimates across Europe (1982–2011). *Global Change Biology*, *20*(11), 3457–3470. https://doi.org/10.1111/gcb.12625

Gharun, M., Hörtnagl, L., Paul-Limoges, E., Ghiasi, S., Feigenwinter, I., Burri, S., et al. (2020). Physiological response of Swiss ecosystems to 2018 drought across plant types and elevation. *Philosophical Transactions of the Royal Society B: Biological Sciences*, *375*(1810), 20190521. https://doi.org/10.1098/rstb.2019.0521

Gibbs, H. K. (2006). *Olson's major world ecosystem complexes ranked by carbon in live vegetation: An updated database using the GLC2000 land cover product (NDP-017b)*. OSTI. Retrieved from https://www.osti.gov/biblio/1389498

Grossiord, C., Buckley, T. N., Cernusak, L. A., Novick, K. A., Poulter, B., Siegwolf, R. T. W., et al. (2020). Plant responses to rising vapor pressure deficit. *New Phytologist*, *226*(6), 1550–1566. https://doi.org/10.1111/nph.16485

Hararuk, O., Obrist, D., & Luo, Y. (2013). Modelling the sensitivity of soil mercury storage to climate-induced changes in soil carbon pools. *Biogeosciences*, *10*(4), 2393–2407. https://doi.org/10.5194/bg-10-2393-2013

Hersbach, H., Bell, B., Berrisford, P., Biavati, G., Horányi, A., Muñoz Sabater, J., et al. (2018). ERA5 hourly data on pressure levels from 1979 to present. In *Copernicus climate change Service (C3S) climate data Store (CDS). Copernicus*. https://doi.org/10.24381/cds.bd0915c6

IPCC. (2021a). Climate change 2021. The physical science basis. Working group I contribution to the sixth assessment report of the intergovernmental panel on climate change. Sixth assessment report. Retrieved from https://www.ipcc.ch/report/ar6/wg1/

IPCC. (2021b). Summary for policymakers. Climate change 2021: The physical science basis. Contribution of working group I to the sixth assessment report of the intergovernmental panel on climate change. Sixth assessment report. Retrieved from https://www.ipcc.ch/report/ar6/wg1/chapter/summary-for-policymakers/

Jacob, D., Teichmann, C., Sobolowski, S., Katragkou, E., Anders, I., Belda, M., et al. (2020). Regional climate downscaling over Europe: Perspectives from the EURO-CORDEX community. *Regional Environmental Change*, *20*(2), 51. https://doi.org/10.1007/s10113-020-01606-9

Jeong, S.-J., Ho, C.-H., Gim, H.-J., & Brown, M. E. (2011). Phenology shifts at start vs. end of growing season in temperate vegetation over the Northern Hemisphere for the period 1982–2008. *Global Change Biology*, *17*(7), 2385–2399. https://doi.org/10.1111/j.1365-2486.2011.02397.x

Jiskra, M., Sonke, J. E., Obrist, D., Bieser, J., Ebinghaus, R., Myhre, C. L., et al. (2018). A vegetation control on seasonal variations in global atmospheric mercury concentrations. *Nature Geoscience*, *1–7*(4), 244–250. https://doi.org/10.1038/s41561-018-0078-8

Jiskra, M., Wiederhold, J. G., Skyllberg, U., Kronberg, R.-M., Hajdas, I., & Kretzschmar, R. (2015). Mercury deposition and re-emission pathways in boreal forest soils investigated with Hg isotope signatures. *Environmental Science & Technology*, *49*(12), 7188–7196. Retrieved from https://pubs.acs.org/doi/10.1021/acs.est.5b00742

Kellomäki, S., Strandman, H., Heinonen, T., Asikainen, A., Venäläinen, A., & Peltola, H. (2018). Temporal and spatial change in diameter growth of boreal scots pine, Norway spruce, and birch under recent-generation (CMIP5) global climate model projections for the 21st century. *Forests*, *9*(3), 118. https://doi.org/10.3390/f9030118

Khan, T., Obrist, D., Agnan, Y., Selin, N. E., & Perlinger, J. A. (2019). Atmosphere-terrestrial exchange of gaseous elemental mercury: Parameterization improvement through direct comparison with measured ecosystem fluxes. *Environmental Sciences: Processes & Impacts*, *21*(10), 1699–1712. https://doi.org/10.1039/C9EM00341J

Körner, C. (2013). Plant–Environment interactions. In A. Bresinsky, C. Körner, J. W. Kadereit, G. Neuhaus, & U. Sonnewald (Eds.), *Strasburger's plant sciences: Including Prokaryotes and Fungi* (pp. 1065–1166). Springer. https://doi.org/10.1007/978-3-642-15518-5_12

Ku, H. (1966). Notes on the use of propagation of error formulas. *Journal of Research of the National Bureau of Standards*, *70C*(4), 263. https://doi.org/10.6028/jres.070c.025

Laacouri, A., Nater, E. A., & Kolka, R. K. (2013). Distribution and uptake dynamics of mercury in leaves of common deciduous tree species in Minnesota U.S.A. *Environmental Science & Technology*, *47*(18), 10462–10470. https://doi.org/10.1021/es401357z

Lagergren, F., & Lindroth, A. (2002). Transpiration response to soil moisture in pine and spruce trees in Sweden. *Agricultural and Forest Meteorology*, *112*(2), 67–85. https://doi.org/10.1016/S0168-1923(02)00060-6

Liu, Y., Liu, G., Wang, Z., Guo, Y., Yin, Y., Zhang, X., et al. (2021). Understanding foliar accumulation of atmospheric Hg in terrestrial vegetation: Progress and challenges. *Critical Reviews in Environmental Science and Technology*, *0*(0), 1–22. https://doi.org/10.1080/10643389.2021.1989235

Lucchesi, R. (2018). *File specification for GEOS FP. GMAO office note No. 4 (version 1.2)*. GMAO. Retrieved from http://gmao.gsfc.nasa.gov/pubs/office_notes

Martínez-Ferri, E., Balaguer, L., Valladares, F., Chico, J. M., & Manrique, E. (2000). Energy dissipation in drought-avoiding and drought-tolerant tree species at midday during the Mediterranean summer. *Tree Physiology*, *20*(2), 131–138. https://doi.org/10.1093/treephys/20.2.131

Mauri, A., Strona, G., & San-Miguel-Ayanz, J. (2017). EU-Forest, a high-resolution tree occurrence dataset for Europe. *Scientific Data*, *4*(1), 160123. https://doi.org/10.1038/sdata.2016.123

Naturvårdsverket. (2023). Informative inventory report Sweden 2023. Submitted under the Convention on Long-Range Transboundary Air Pollution. Swedish Environmental Protection Agency. Retrieved from https://www.google.com/url?sa=t&rct=j&q=&esrc=s&source=web&cd=&cad=rja&uact=8&ved=2ahUKEwje25TllN-BAxU8bvEDHVWoBUMQFnoECA8QAQ&url=https%3A%2F%2Fwww.naturvardsverket.se%2F494814%2Fcontentassets%2Fa793266c97e54f95806a9793fad82217%2Finformative-inventory-report-sweden-2023.pdf&usg=AOvVaw3o-Huesej4-AnJVqESV8xQ&opi=89978449

Norby, R. J., & Zak, D. R. (2011). Ecological lessons from free-air CO_2 enrichment (FACE) experiments. *Annual Review of Ecology, Evolution, and Systematics*, *42*(1), 181–203. https://doi.org/10.1146/annurev-ecolsys-102209-144647

Obrist, D., Agnan, Y., Jiskra, M., Olson, C. L., Colegrove, D. P., Hueber, J., et al. (2017). Tundra uptake of atmospheric elemental mercury drives Arctic mercury pollution. *Nature*, *547*(7662), 201–204. https://doi.org/10.1038/nature22997

Obrist, D., Roy, E. M., Harrison, J. L., Kwong, C. F., Munger, J. W., Moosmüller, H., et al. (2021). Previously unaccounted atmospheric mercury deposition in a midlatitude deciduous forest. *PNAS*, *118*(29). https://doi.org/10.1073/pnas.2105477118

Oksanen, E., Lihavainen, J., Keinänen, M., Keski-Saari, S., Kontunen-Soppela, S., Sellin, A., & Sõber, A. (2019). Northern forest trees under increasing atmospheric humidity. In F. M. Cánovas, U. Lüttge, R. Matyssek, & H. Pretzsch (Eds.), *Progress in botany* (Vol. 80, pp. 317–336). Springer International Publishing. https://doi.org/10.1007/124_2017_15

Panagos, P., Jiskra, M., Borrelli, P., Liakos, L., & Ballabio, C. (2021). Mercury in European topsoils: Anthropogenic sources, stocks and fluxes. *Environmental Research*, *201*, 111556. https://doi.org/10.1016/j.envres.2021.111556

Panek, J. A., & Goldstein, A. H. (2001). Response of stomatal conductance to drought in ponderosa pine: Implications for carbon and ozone uptake. *Tree Physiology*, *21*(5), 337–344. https://doi.org/10.1093/treephys/21.5.337

Papula, L. (2003). Mathematische Formelsammlung für Ingenieure und Naturwissenschaftler (8th ed.).

Pleijel, H., Klingberg, J., Nerentorp, M., Broberg, M. C., Nyirambangutse, B., Munthe, J., & Wallin, G. (2021). Mercury accumulation in leaves of different plant types—The significance of tissue age and specific leaf area. *Biogeosciences*, *18*(23), 6313–6328. https://doi.org/10.5194/bg-18-6313-2021

Rea, A. W., Lindberg, S. E., Scherbatskoy, T., & Keeler, G. J. (2002). Mercury accumulation in foliage over time in two northern mixed-hardwood forests. *Water, Air, & Soil Pollution*, *133*(1/4), 49–67. https://doi.org/10.1023/a:1012919731598

Rutter, A. P., Schauer, J. J., Shafer, M. M., Creswell, J. E., Olson, M. R., Robinson, M., et al. (2011). Dry deposition of gaseous elemental mercury to plants and soils using mercury stable isotopes in a controlled environment. *Atmospheric Environment*, *45*(4), 848–855. https://doi.org/10.1016/j.atmosenv.2010.11.025

Samaniego, L., Thober, S., Kumar, R., Wanders, N., Rakovec, O., Pan, M., et al. (2018). Anthropogenic warming exacerbates European soil moisture droughts. *Nature Climate Change*, *8*(5), 421–426. https://doi.org/10.1038/s41558-018-0138-5

Selin, N. E., Jacob, D. J., Yantosca, R. M., Strode, S., Jaeglé, L., & Sunderland, E. M. (2008). Global 3-D land-ocean-atmosphere model for mercury: Present-day versus preindustrial cycles and anthropogenic enrichment factors for deposition. *Global Biogeochemical Cycles*, *22*(2). https://doi.org/10.1029/2007GB003040

Smith-Downey, N. V., Sunderland, E. M., & Jacob, D. J. (2010). Anthropogenic impacts on global storage and emissions of mercury from terrestrial soils: Insights from a new global model. *Journal of Geophysical Research*, *115*(G3), G03008. https://doi.org/10.1029/2009JG001124

Sonke, J. E., Angot, H., Zhang, Y., Poulain, A., Björn, E., & Schartup, A. (2023). Global change effects on biogeochemical mercury cycling. *Ambio*, *52*(5), 853–876. https://doi.org/10.1007/s13280-023-01855-y

Stocker, B. D., Zscheischler, J., Keenan, T. F., Prentice, I. C., Seneviratne, S. I., & Peñuelas, J. (2019). Drought impacts on terrestrial primary production underestimated by satellite monitoring. *Nature Geoscience*, *12*(4), 264–270. https://doi.org/10.1038/s41561-019-0318-6

Tørseth, K., Aas, W., Breivik, K., Fjæraa, A. M., Fiebig, M., Hjellbrekke, A. G., et al. (2012). Introduction to the European Monitoring and Evaluation Programme (EMEP) and observed atmospheric composition change during 1972-2009. *Atmospheric Chemistry and Physics*, *12*(12), 5447–5481. https://doi.org/10.5194/acp-12-5447-2012

Wang, Q., Tenhunen, J., Dinh, N., Reichstein, M., Otieno, D., Granier, A., & Pilegarrd, K. (2005). Evaluation of seasonal variation of MODIS derived leaf area index at two European deciduous broadleaf forest sites. *Remote Sensing of Environment*, *96*(3–4), 475–484. https://doi.org/10.1016/j.rse.2005.04.003

Wang, R., Chen, J. M., Liu, Z., & Arain, A. (2017). Evaluation of seasonal variations of remotely sensed leaf area index over five evergreen coniferous forests. *ISPRS Journal of Photogrammetry and Remote Sensing*, *130*, 187–201. https://doi.org/10.1016/j.isprsjprs.2017.05.017

Wang, Y., Jacob, D. J., & Logan, J. A. (1998). Global simulation of tropospheric O_3-NO_x -hydrocarbon chemistry: 1. Model formulation. *Journal of Geophysical Research*, *103*(D9), 10713–10725. https://doi.org/10.1029/98JD00158

Wesely, M. L. (2007). Parameterization of surface resistances to gaseous dry deposition in regional-scale numerical models. *Atmospheric Environment*, *41*, 52–63. https://doi.org/10.1016/j.atmosenv.2007.10.058

Wohlgemuth, L., Osterwalder, S., Joseph, C., Kahmen, A., Hoch, G., Alewell, C., & Jiskra, M. (2020). A bottom-up quantification of foliar mercury uptake fluxes across Europe. *Biogeosciences*, *17*(24), 6441–6456. https://doi.org/10.5194/bg-17-6441-2020

Wohlgemuth, L., Rautio, P., Ahrends, B., Russ, A., Vesterdal, L., Waldner, P., et al. (2022). Physiological and climate controls on foliar mercury uptake by European tree species. *Biogeosciences*, *19*(5), 1335–1353. https://doi.org/10.5194/bg-19-1335-2022

Wu, Z., Wang, X., Chen, F., Turnipseed, A. A., Guenther, A. B., Niyogi, D., et al. (2011). Evaluating the calculated dry deposition velocities of reactive nitrogen oxides and ozone from two community models over a temperate deciduous forest. *Atmospheric Environment*, *45*(16), 2663–2674. https://doi.org/10.1016/j.atmosenv.2011.02.063

Yuan, H., Dai, Y., Xiao, Z., Ji, D., & Shangguan, W. (2011). Reprocessing the MODIS Leaf Area Index products for land surface and climate modelling. *Remote Sensing of Environment*, *115*(5), 1171–1187. https://doi.org/10.1016/j.rse.2011.01.001

Yuan, W., Sommar, J., Lin, C.-J., Wang, X., Li, K., Liu, Y., et al. (2019a). Stable isotope evidence shows re-emission of elemental mercury vapor occurring after reductive loss from foliage. *Environmental Science & Technology*, *53*(2), 651–660. https://doi.org/10.1021/acs.est.8b04865

Yuan, W., Zheng, Y., Piao, S., Ciais, P., Lombardozzi, D., Wang, Y., et al. (2019b). Increased atmospheric vapor pressure deficit reduces global vegetation growth. *Science Advances*, *5*(8). https://doi.org/10.1126/sciadv.aax1396

Zhang, H., Holmes, C., & Wu, S. (2016). Impacts of changes in climate, land use and land cover on atmospheric mercury. *Atmospheric Environment*, *141*, 230–244. https://doi.org/10.1016/j.atmosenv.2016.06.056

Zhang, L., Wright, L. P., & Blanchard, P. (2009). A review of current knowledge concerning dry deposition of atmospheric mercury. *Atmospheric Environment*, *43*(37), 5853–5864. https://doi.org/10.1016/j.atmosenv.2009.08.019

Zhou, J., Bollen, S. W., Roy, E. M., Hollinger, D. Y., Wang, T., Lee, J. T., & Obrist, D. (2023). Comparing ecosystem gaseous elemental mercury fluxes over a deciduous and coniferous forest. *Nature Communications*, *14*(1), 2722. https://doi.org/10.1038/s41467-023-38225-x

Zhou, J., & Obrist, D. (2021). Global mercury assimilation by vegetation. *Environmental Science & Technology*, *55*(20), 14245–14257. https://doi.org/10.1021/acs.est.1c03530

Zhou, J., Obrist, D., Dastoor, A., Jiskra, M., & Ryjkov, A. (2021). Vegetation uptake of mercury and impacts on global cycling. *Nature Reviews Earth & Environment*, *2*(4), 1–16. https://doi.org/10.1038/s43017-021-00146-y

Zweifel, R., Rigling, A., & Dobbertin, M. (2009). Species-specific stomatal response of trees to drought—A link to vegetation dynamics? *Journal of Vegetation Science*, *20*(3), 442–454. https://doi.org/10.1111/j.1654-1103.2009.05701.x

Zweifel, R., Steppe, K., & Sterck, F. J. (2007). Stomatal regulation by microclimate and tree water relations: Interpreting ecophysiological field data with a hydraulic plant model. *Journal of Experimental Botany*, *58*(8), 2113–2131. https://doi.org/10.1093/jxb/erm050